ADVANCES IN ATMOSPHERIC SCIENCES, VOL. 30, NO. 3, 2013, 674–683

Preliminary Evaluations of FGOALS-g2 for Decadal Predictions

WANG Bin*[1,2] (王 斌), LIU Mimi[1] (刘咪咪), YU Yongqiang[1] (俞永强), LI Lijuan[1] (李立娟), LIN Pengfei[1] (林鹏飞), DONG Li[1] (董 理), LIU Li[2] (刘 利), LIU Jiping[1] (刘骥平), HUANG Wenyu[2] (黄文誉), XU Shiming[2] (徐世明), SHEN Si[1] (申 思), PU Ye[1] (普 业), XUE Wei[2] (薛 巍), XIA Kun[2] (夏 坤), WANG Yong[1] (王 勇), SUN Wenqi[1] (孙文奇), HU Ning[1] (胡 宁), HUANG Xiaomeng[2] (黄小猛), LIU Hailong[1] (刘海龙), ZHENG Weipeng[1] (郑伟鹏), WU Bo[1] (吴 波), ZHOU Tianjun[1] (周天军), and YANG Guangwen[2] (杨广文)

[1] *State Key Laboratory of Numerical Modeling for Atmospheric Sciences and Geophysical Fluid Dynamics, Institute of Atmospheric Physics, Chinese Academy of Sciences, Beijing* 100029

[2] *Ministry of Education Key Laboratory for Earth System Modeling, Center for Earth System Science, Tsinghua University, Beijing* 100084

(Received 25 April 2012; revised 9 August 2012)

ABSTRACT

The Flexible Global Ocean-Atmosphere-Land System model, Grid-point Version 2 (FGOALS-g2) for decadal predictions, is evaluated preliminarily, based on sets of ensemble 10-year hindcasts that it has produced. The results show that the hindcasts were more accurate in decadal variability of SST and surface air temperature (SAT), particularly in that of Niño3.4 SST and China regional SAT, than the second sample of the historical runs for 20th-century climate (the control) by the same model. Both the control and the hindcasts represented the global warming well using the same external forcings, but the control overestimated the warming. The hindcasts produced the warming closer to the observations. Performance of FGOALS-g2 in hindcasts benefits from more realistic initial conditions provided by the initialization run and a smaller model bias resulting from the use of a dynamic bias correction scheme newly developed in this study. The initialization consists of a 61-year nudging-based assimilation cycle, which follows on the control run on 01 January 1945 with the incorporation of observation data of upper-ocean temperature and salinity at each integration step in the ocean component model, the LASG IAP Climate System Ocean Model, Version 2 (LICOM2). The dynamic bias correction is implemented at each step of LICOM2 during the hindcasts to reduce the systematic biases existing in upper-ocean temperature and salinity by incorporating multi-year monthly mean increments produced in the assimilation cycle. The effectiveness of the assimilation cycle and the role of the correction scheme were assessed prior to the hindcasts.

Key words: decadal prediction, initialization, dynamic bias correction, evaluation

Citation: Wang, B., and Coauthors, 2013: Preliminary evaluations of FGOALS-g2 for decadal prediction. *Adv. Atmos. Sci.*, **30**(3), 674–683, doi: 10.1007/s00376-012-2084-x.

1. Introduction

Improving decadal predictions for global and regional climate changes is of scientific significance and has important societal implications (Meehl et al., 2009). These predictions may better present extremes due to naturally occurring decadal variability and may be useful in risk and cost-benefit analyses of new investments in large-scale infrastructure that are generally proposed according to decadal time scales. However, decadal predictions are technically challenging. These predictions differ from seasonal forecasts that are initialized from observed climate system states and climate projections that generally follow long-term

*Corresponding author: WANG Bin, wab@tsinghua.edu.cn

spin-ups of coupled climate/earth system models. The methodology to make decadal predictions is in its infancy. Like seasonal prediction strategies, initializing the models using full observations (as opposed to anomalies) may lead to drifts in decadal predictions from the observations toward an imperfect model climate (Troccoli and Palmer, 2007). These drifts are generally produced by the systematic biases between the model simulations and observations. Therefore, initializing the models and making bias corrections are very important for decadal predictions.

The drift problem was reduced greatly when Schneider et al. (1999) proposed an initialization scheme that assimilates anomalies rather than absolute values of observations. Sets of hindcast experiments initialized with observation anomalies by Pierce et al. (2004), Smith et al. (2007) and Keenlyside et al. (2008) also showed that decadal hindcasts were better than simulations without initializations under the same radiative forcing. The difficulties of initializing the ocean state become more serious due to the lack of observations on sea subsurface. For this reason, Pohlmann et al. (2009) initialized their decadal predictions with anomalies of ocean temperature and salinity from re-analysis data and found that the accuracy of the hindcasts were extended to decadal time scale. Particularly, their hindcasts represented the North Atlantic Oscillation (NAO) well. However, when initial conditions (ICs) that incorporate observation anomalies are used, a coupled model that is incompatible with this state may quickly "forget" the details of the initial conditions because of model errors (Barnett et al., 2004; Pierce et al., 2004) that cannot be reduced by the assimilation of anomaly observations. To alleviate model errors, much research has been conducted, including the development of a statistical method to remove initial biases that may cause climate drifts (Cherupin et al., 2005; Dee, 2005), the estimation of model parameters using observations through the ensemble adjustment Kalman filter (EAKF) to reduce hindcast/forecast errors caused by "initial shocks" (Zhang, 2011), and the incremental analysis update (IAU) data assimilation approach with which Mochizuki et al. (2010) hindcast the Pacific Decadal Oscillation (PDO) successfully.

In this study, a dynamic bias correction scheme was newly developed to alleviate drifts caused by the use of the absolute values of observations in the nudging-based initialization, which is introduced in section 2, following a brief description of the coupled model and assimilation method used in this study. The experiment design is then given in section 3, followed by the preliminary evaluations in section 4. Finally, the summary and conclusions of this paper are presented in section 5.

2. Methodology

2.1 *Model description*

The climate system model used in this study was the Flexible Global Ocean-Atmosphere-Land System model, Grid-point Version 2 (FGOALS-g2), which is one of the CMIP5 (Coupled Model Intercomparison Project Phase 5) models (http://pcmdi3.llnl.gov/esgcet/home.htm) mainly developed jointly by the State Key Laboratory of Numerical Modeling for Atmospheric Sciences and Geophysical Fluid Dynamics (LASG), Institute of Atmospheric Physics (IAP), Chinese Academy of Science (CAS), and the Center for Earth System Science (CESS), Tsinghua University. It couples four components, including the Grid-point Atmospheric Model of IAP LASG, version 2 (GAMIL2), the LASG IAP Climate Ocean system Model, version 2 (LICOM2); the Community Land Model, version 3 (CLM3) of National Center for Atmospheric Research (NCAR); and the Los Alamos Sea Ice Model (CICE), improved version 1.0 by LASG (CICE_LASG1.0: Wang, 2009; Song and Liu, 2012[a]), through the NCAR Coupler Version 6 (CPL6) which computes and exchanges the heat flux, momentum and fresh water flux among the component models without any flux correction or adjustment. The grid resolution of this couple model is $2.8^\circ \times 2.8^\circ$ L26 in the atmosphere (Wang et al., 2004; Li et al., 2012a; Li et al., 2013a) and $1^\circ \times (0.5^\circ - 1^\circ)$ L30 in the ocean (Liu et al., 2012). The sea-ice model has five levels in the vertical direction. Because the coupler requests that the ocean and sea-ice models have the same grids, the horizontal resolution of the sea-ice model was modified to match that of LICOM2. The horizontal resolution of the land surface model was also modified to match that of GAMIL2. For more detailed descriptions of the coupled model, please refer to Li et al. (2013b).

2.2 *Assimilation scheme for initialization*

Initialization is one of the essential steps of decadal prediction; in this step observational information is spread to the deep ocean and other model variables without observations, using an assimilation approach. Because the initialization of a coupled model requires a long cycle of assimilation, the computing efficiency of the chosen assimilation scheme must be sufficiently considered. For this reason, the nudging-based

[a]Song, M., and J. Liu, 2012: Sensitivity of sea ice simulations to two different snow/ice albedo parameterizations. *Climate dyn.*, submitted.

assimilation scheme, a simplified scheme of three-dimensional variational data assimilation (3DVAR), was used to initialize the simulations in this study.

3DVAR obtains its initial analysis $\boldsymbol{x}_\mathrm{a}$ through minimizing a cost function:

$$\begin{cases} J(\boldsymbol{x}_\mathrm{a}) = \min\limits_{\boldsymbol{x}} J(\boldsymbol{x}) \\ J(\boldsymbol{x}) = \dfrac{1}{2}(\boldsymbol{x}-\boldsymbol{x}_\mathrm{b})^\mathrm{T}\boldsymbol{B}^{-1}(\boldsymbol{x}-\boldsymbol{x}_\mathrm{b}) + \\ \qquad\qquad \dfrac{1}{2}(\boldsymbol{H}(\boldsymbol{x})-\boldsymbol{y}_\mathrm{obs})^\mathrm{T}\boldsymbol{O}^{-1}(\boldsymbol{H}(\boldsymbol{x})-\boldsymbol{y}_\mathrm{obs}) \end{cases}, \tag{1}$$

where $\boldsymbol{B}$ is background error covariance matrix, $\boldsymbol{O}$ is observational error covariance matrix that is generally diagonal, $\boldsymbol{x}_\mathrm{b}$ is background, $\boldsymbol{y}_\mathrm{obs}$ is observation, and $\boldsymbol{H}$ is the observational operator. If the observational variable $\boldsymbol{y} = \boldsymbol{H}(\boldsymbol{x})$ is the same as the control variable $\boldsymbol{x}$ (i.e., $\boldsymbol{H} = \boldsymbol{I}$ and $\boldsymbol{x}_\mathrm{obs} = \boldsymbol{y}_\mathrm{obs}$) and the matrices $\boldsymbol{B}$ and $\boldsymbol{O}$ are all diagonal with constant variances at the diagonal line (i.e., $\boldsymbol{B} = \alpha_\mathrm{b}^2\boldsymbol{I}$ and $\boldsymbol{O} = \alpha_\mathrm{o}^2\boldsymbol{I}$, where α_b^2 and α_o^2 are respectively the mean variances of background and observational errors), the cost function of 3DVAR defined in Eq. (1) is then simplified into the following formula:

$$J(\boldsymbol{x}) = \frac{\alpha_\mathrm{b}^{-2}}{2}(\boldsymbol{x}-\boldsymbol{x}_\mathrm{b})^\mathrm{T}(\boldsymbol{x}-\boldsymbol{x}_\mathrm{b}) + \frac{\alpha_\mathrm{o}^{-2}}{2}(\boldsymbol{x}-\boldsymbol{x}_\mathrm{obs})^\mathrm{T}(\boldsymbol{x}-\boldsymbol{x}_\mathrm{obs}), \tag{2}$$

which can be regarded as the cost function of the nudging-based assimilation. It is easy to obtain the initial analysis by minimizing this cost function:

$$\boldsymbol{x}_\mathrm{a} = \boldsymbol{x}_\mathrm{b} + \alpha(\boldsymbol{x}_\mathrm{obs} - \boldsymbol{x}_\mathrm{b}) \left(\text{where } \alpha = \frac{\alpha_\mathrm{b}^2}{\alpha_\mathrm{b}^2 + \alpha_\mathrm{o}^2}\right). \tag{3}$$

If a model integration from n-th step to n+1-th step is expressed into

$$\boldsymbol{x}_n + 1 = \boldsymbol{x}_n + \tau\boldsymbol{L}(\boldsymbol{x}_n), \tag{4}$$

the nudging-based assimilation for this step can be formulated as

$$\begin{cases} \boldsymbol{x}_{\mathrm{a},n} = \boldsymbol{x}_n + \alpha(\boldsymbol{x}_{\mathrm{obs},n} - \boldsymbol{x}_n) \\ \boldsymbol{x}_{n+1} = \boldsymbol{x}_{\mathrm{a},n} + \tau\boldsymbol{L}(\boldsymbol{x}_{\mathrm{a},n}) \end{cases}, \tag{5}$$

where $\boldsymbol{L}$ is the tendency of the model, τ is the time step size, and α is the nudging coefficient. To improve the consistence between the observation and model background, an extra iteration with m sub-steps is used to assimilate the same observation at each model integration step:

$$\begin{cases} \boldsymbol{x}_{\mathrm{b},n,0} = \boldsymbol{x}_n \\ \begin{cases} \boldsymbol{x}_{\mathrm{a},n,k} = \boldsymbol{x}_{\mathrm{b},n,k} + \dfrac{\alpha}{m}(\boldsymbol{x}_{\mathrm{obs},n} - \boldsymbol{x}_{\mathrm{b},n,k}) \\ \boldsymbol{x}_{\mathrm{b},n,k+1} = \boldsymbol{x}_{\mathrm{a},n,k} + \dfrac{\tau}{m}\boldsymbol{L}(\boldsymbol{x}_{\mathrm{a},n,k}) \end{cases} \\ \qquad\qquad (k = 0, 1, \cdots, m-1) \\ \boldsymbol{x}_{n+1} = \boldsymbol{x}_{\mathrm{b},n,m} \end{cases}. \tag{6}$$

In this study, the number of substep m is set to be 2, so the related computation is not very time-consuming.

2.3 *Dynamic bias correction in decadal prediction*

The different assimilation strategies used in initializations all have pros and cons. Initializing the model simulations with anomaly observations can reduce climate drifts in decadal predictions, but it is difficult to remove the initial biases. Initializing with full observations can alleviate the model biases in the first prediction year, but this may lead to drifts in the following prediction years from the observations toward an imperfect model climate. In this study, full observations were directly assimilated during the initialization, and a dynamic bias correction scheme was proposed to reduce the climate drifts in decadal predictions.

From Eq. (5) or (6), it can be easily proven that the analysis $\boldsymbol{x}_{\mathrm{a},n}$ ($\boldsymbol{x}_{\mathrm{a},n,k}$) was closer to the observation $\boldsymbol{x}_{\mathrm{obs},n}$ than the background $\boldsymbol{x}_{\mathrm{b},n}$ ($\boldsymbol{x}_{\mathrm{b},n,k}$) model prediction. Therefore, the analysis increment $\boldsymbol{x'}_{\mathrm{a},n} = \alpha(\boldsymbol{x}_{\mathrm{obs},n} - \boldsymbol{x}_{\mathrm{b},n})$ ($\boldsymbol{x'}_{\mathrm{a},n,k} = \alpha/m(\boldsymbol{x}_{\mathrm{obs},n} - \boldsymbol{x}_{\mathrm{b},n,k})$) can alleviate the error between the prediction and observations. Without question, the multi-year monthly mean analysis increments $\bar{\boldsymbol{x}}'_{\mathrm{a,mon}}$ (mon$= 1, 2, \ldots, 12$) during the initialization can reduce the model bias in mean annual cycle (MAC) during this period. They also reduce the MAC bias in hindcasts/forecasts to some extent, because the same model was used in both the initialization and hindcast/forecast. Therefore, the following dynamic bias correction scheme for decadal prediction based on Eq. (5) or (6) was proposed:

$$\begin{cases} \boldsymbol{x}_{\mathrm{a},n} = \boldsymbol{x}_n + \bar{\boldsymbol{x}}'_{\mathrm{a},n} \\ \boldsymbol{x}_{n+1} = \boldsymbol{x}_{\mathrm{a},n} + \tau\boldsymbol{L}(\boldsymbol{x}_{\mathrm{a},n}) \end{cases}, \tag{7}$$

or

$$\begin{cases} \boldsymbol{x}_{\mathrm{b},n,0} = \boldsymbol{x}_n \\ \begin{cases} \boldsymbol{x}_{\mathrm{a},n,k} = \boldsymbol{x}_{\mathrm{b},n,k} + \dfrac{1}{m}\bar{\boldsymbol{x}}'_{\mathrm{a},n} \\ \boldsymbol{x}_{\mathrm{b},n,k+1} = \boldsymbol{x}_{\mathrm{a},n,k} + \dfrac{\tau}{m}\boldsymbol{L}(\boldsymbol{x}_{\mathrm{a},n,k}) \end{cases} \\ \qquad\qquad (k = 0, 1, \cdots, m-1) \\ \boldsymbol{x}_{n+1} = \boldsymbol{x}_{\mathrm{b},n,m} \end{cases}, \tag{8}$$

where $\bar{\boldsymbol{x}}'_{\mathrm{a},n}$ is obtained from linear time interpolation of $\bar{\boldsymbol{x}}'_{\mathrm{a,mon}}$ (mon$= 1, 2, \ldots, 12$) at the time of each integration step.

3. Experiment design

3.1 *Initialization experiment*

The initialization experiment (simply "ASSIM", hereinafter) consisted of a 61-year (1945–2005) assimilation cycle performed to provide the ICs for the hindcast and forecast experiments initiated any time between 1955 and 2005. This model run actually follows one of the historical runs (the second sample) for 20th century climate (marked "CTRL" as the control run) at 0000 UTC on 01 January 1945. ASSIM used the same external forcings as CTRL, however, in ASSIM the monthly mean upper-ocean temperature (T) and salinity (S) of FGOALS-g2 are relaxed toward the ds285.3 analyzed data (Isii et al., 2006) over the entire period 1945–2005 using the scheme shown in Eq. (6). A linear interpolation was used to derive intermonthly observations. Because the inconsistency in sea-ice cover between the model and the observations usually results in unfavorable temperature and salinity variations over the polar regions in the initialization, assimilation analyses were not performed at the grid points where sea-ice existed in the model. With regard to a grid point located away from the modeled sea ice within a distance of 10° in latitude, the analysis increment was dampened in proportion to the distance between the point and sea ice [a method similar to that used by Mochizuki et al., 2010]. The nudging coefficient in Eq. (5) or (6) was set as $\alpha = \sigma(\theta)\alpha_0$, where θ is the latitude and $\alpha_0 = (\tau_{\mathrm{T-S}}/3600)/(30\times24)$ (the subscript "T-S" means "for the temperature and salinity equations"), considering that the observation are monthly mean data. The assimilations were performed at each step of the temperature and salinity integration in the ocean model with the time step-size $\tau_{\mathrm{T-S}}$, and $\sigma(\theta)$ was set as the following:

$$\sigma(\theta) = \begin{cases} \dfrac{\pi - 2\,|\theta|}{30\pi} & \dfrac{\pi}{3} < |\theta| \leqslant \dfrac{\pi}{2} \\ \dfrac{1}{90} + \dfrac{29}{15\pi}(\pi - 3\,|\theta|) & \dfrac{5\pi}{18} < |\theta| \leqslant \dfrac{\pi}{3} \\ \dfrac{1}{2} + \dfrac{1}{9\pi}(\pi - 9\,|\theta|) & \dfrac{\pi}{9} < |\theta| \leqslant \dfrac{5\pi}{18} \\ \dfrac{1}{2} & -\dfrac{\pi}{9} \leqslant \theta \leqslant \dfrac{\pi}{9} \end{cases} . \quad (9)$$

3.2 *Hindcast experiments*

To evaluate the skill of FGOALS-g2 in decadal predictions, hindcast experiments were designed for the period 1955–2001. Using the ICs provided by ASSIM and the same external forcings (e.g., CO_2 and other greenhouse gases as CTRL), ten sets of 10-year-long, three-member ensemble hindcast experiments were conducted every five years between 1955 and 2001 (referred to as 'HCSTs'). Member 1 (simply 'HCST-r1', hereafter) started the hindcasts on 01 January of 1956 to 2001 with the five-year time interval. Member 2 (marked 'HCST-r2') and Member 3 ('HCST-r3') respectively initiate from 01 November and 01 September from 1955 to 2000 every five years. All three members used the dynamic bias correction scheme to reduce climate drifts caused by incorporating full observations into ICs. To compare the skill of FGOALS-g2 in decadal predictions with and without the dynamic correction scheme, an extra hindcast experiment was performed using the same ICs as Member 1 but without the dynamic correction (referred to as 'HCST-r1-b').

Due to the insufficient ensemble samples, the results from the hindcast experiments were post-processed as 10-year-averaged fields; then the decadal variability was evaluated. For the analyses on climatology and mean annual cycle of SST, 45-year datasets from 1961 to 2005 were adopted; they consisted of the last five-year predictions from the 10 sets of hindcast experiments.

3.3 *Observations*

The observational data used in this study ('OBS' in the figures) for comparison with HCST, ASSIM, and CTRL simulations included the ds285.3 analyzed data (Isii et al., 2006), the Hadley Centre-Climate Research Unit gridded surface temperature dataset (HadCRUT3v; Brohan et al., 2006), and Hadley Centre Sea Ice and Sea Surface Temperature data set (HadISST; Rayner et al., 2003). For the detail information about these datasets, please refer to the following websites:

(1) http://dss.ucar.edu/datasets/ds285.3/ (for the ds285.3 dataset)

(2) http://www.metoffice.gov.uk/hadobs/hadisst/ (for the HadISST dataset)

(3) http://www.metoffice.gov.uk/hadobs/ (for the HadCRUT3v dataset)

4. Preliminary evaluations

4.1 *Climatology of SST*

Warm pools are mainly located in the western Pacific and Northern Indian Ocean according to observation data (Fig. 1a). They play an important role in the global climate system; they significantly impact climate change and extreme climate in Asian and Pacific regions, due to the huge calorific capacity. However, very few state-of-the-art coupled climate system models (CSMs) in the world can well simulate the range and intensity of the warm pools currently. There are

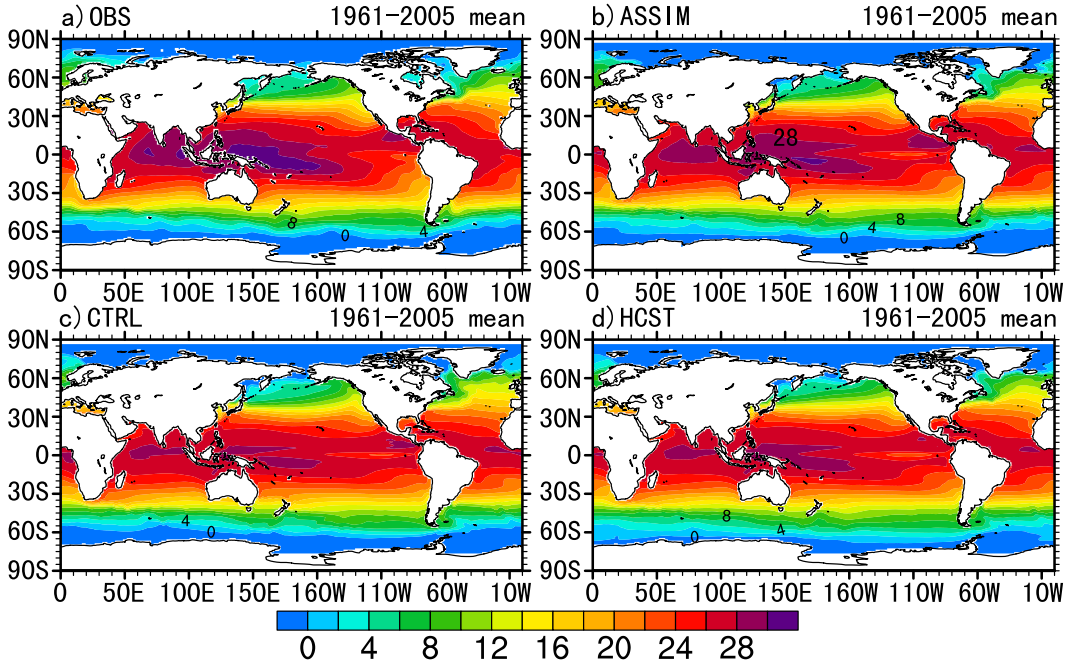

Fig. 1. Horizontal distributions of annual mean SST (1961–2005) in (a) the observation data, (b) initialization experiment, (c) historic run, and (d) the hindcast experiment. The dataset ds285.3 (Isii et al., 2006) was used for the observation data. The units of SST are °C.

some common defects in model simulations, e.g., westward extension of equatorial Pacific cold tongue and narrow distribution in the Indian Ocean, which can also be easily found in CTRL by FGOALS-g2 (Fig. 1c). The range and intensity of the warm pools were significantly improved in ASSIM (Fig. 1b), although there was still a westward extension of Pacific cool tongue. Benefiting from the ICs provided by ASSIM, HCST also slightly improved the range of the Pacific warm pool and alleviated the westward extension of Pacific cool tongue (Fig. 1d).

To investigate the role of the dynamic correction scheme in HCST, the multi-year annual mean SST presented in HCST-r1 was compared with that in HCST-r1-b. As shown in Fig. 2, the warm pool produced by HCST-r1-b without the dynamic correction scheme was much smaller than that of HCST-r1, and the regions enclosed by the contours of 28°C SST almost disappeared. These regions were represented better by HCST-r1, which used the correction scheme. Therefore, the dynamic correction scheme can alleviate the cool drifts and improve the skill of the hindcast on climatological mean of SST.

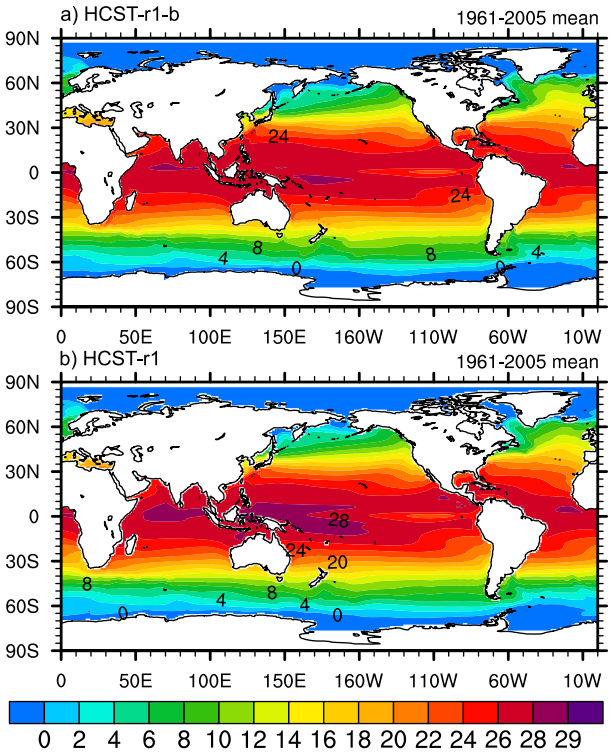

Fig. 2. Horizontal distributions of annual mean SST (1961–2005) in the hindcast sample 1 (a) without and (b) with the dynamic correction scheme. The units of SST are °C.

4.2 *Annual cycle of SST*

The annual cycle of SST is one of the most important physical parameters of the ocean influencing the atmosphere, which directly responds to the annual cy-

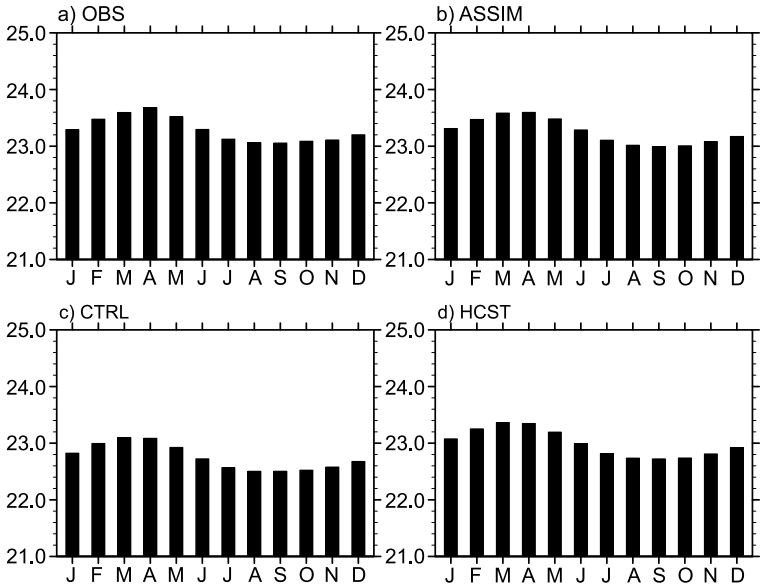

Fig. 3. Mean annual cycle of SST (1961–2005) presented in the (a) observation data, (b) initialization experiment, (c) historical run, and (d) hindcast experiments. The units of SST at the y-axis are °C.

cle of incident solar radiation. It is also the important background of El Niño/Southern Oscillation (ENSO). Therefore, to accurately present the annual cycle of SST is very important for overall performance of the coupled model. In this study, the ability of FGOALS-g2 to represent the 1961–2005 multi-year mean annual cycle of SST in the region between 50°S and 50°N,

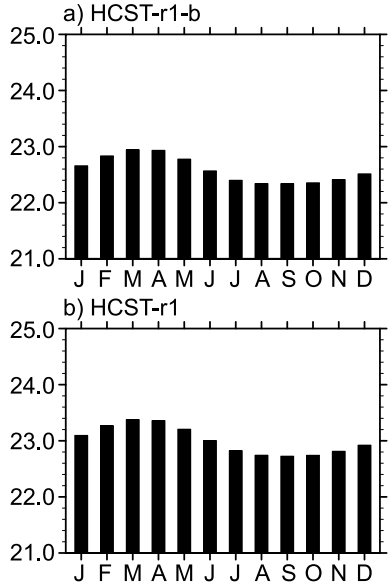

Fig. 4. Mean annual cycle of SST (1961–2005) presented in the hindcast sample 1 (a) without and (b) with the dynamic correction scheme. The units of SST at the y-axis are °C.

where more information of the observations was incorporated into the model run with larger nudging coefficients according to Eq. (9), was investigated. The observations showed that SST reached the highest in April and the lowest in September, with an amplitude of ∼0.63°C (Fig. 3a). Both CTRL and HCST basically replicated this feature, but they all had negative biases that underestimated the SST in each month (Figs. 3c and d). Compared with CTRL, HCST reduced the bias obviously. ASSIM presented the annual cycle of SST the best, nearly matching the observations, with a very small negative bias (Fig. 3b). However, using the same ICs from ASSIM, HCST-r1-b did not alleviate the bias in CTRL and became even worse (Fig. 4a), while HCST-r1 performed as well as HCST (Fig. 4b). Positive roles of the dynamic correction scheme in presenting both the climatology and the mean annual cycle of SST preliminarily verified its feasibility and practicality. Thus we mainly focused on evaluating the skill of HCST in the remainder of the study.

4.3 *Decadal variations of sea surface temperature anomaly*

The skill of FGOALS-g2 to simulate variations of the globally averaged SST anomaly (SSTA) on decadal timescale was analyzed next. As Fig. 5 shows, the model rendered a skillful simulation in CTRL, whose correlation coefficient with the observation was as high as 0.992. The incorporation of SST and salinity data made ASSIM even better in terms of both the correlation coefficient (CC=0.997) and the root mean square

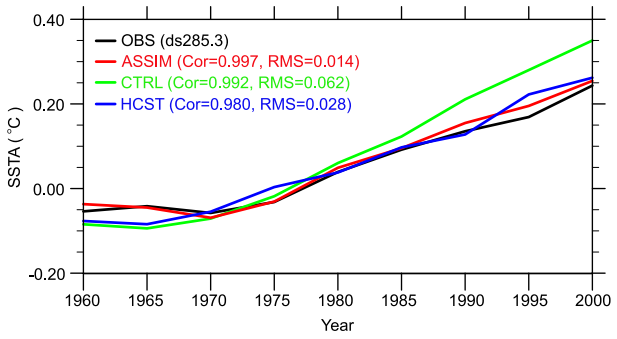

Fig. 5. Decadal variations of globally averaged SST anomaly (SSTA) in the observation data (black), initialization experiment (red), historic run (green), and hindcast experiments (blue). The dataset ds285.3 (Isii et al., 2006) was used for the observation data. The units of SST are °C.

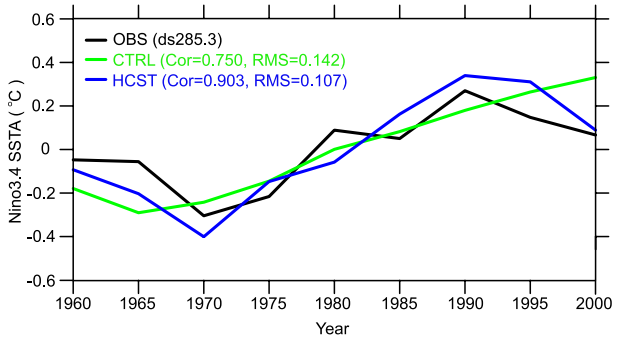

Fig. 6. Decadal variations of Niño3.4 index in the observation data (black), initialization experiment (red), historic run (green), and hindcast experiments (blue). The dataset ds285.3 (Isii et al., 2006) was used for the observation data. The units of Niño3.4 index are °C.

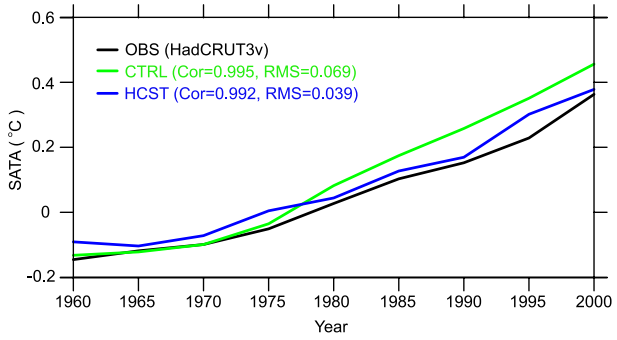

Fig. 7. Decadal variations of globally averaged surface air temperature (SAT) in the observation data (black), historic run (green), and hindcast experiments (blue). The HadCRUT3v dataset (Brohan et al., 2006) was used for the observation data. The units of SAT are °C.

error (RMSE=0.014) that was much less than 0.062 in CTRL. However, overestimations of global ocean warming after 1980 were observed in CTRL. With the high-quality ICs from ASSIM, HCST obviously alleviated the overestimations (Fig. 5), with a much smaller RMSE (0.028) but a very slightly lower correlation coefficient than in CTRL. The improvements of both the climatology and decadal variations of SST in ASSIM and HCST indicate the effectiveness of the initialization and its positive role on and the important contribution of the dynamic bias correction to decadal prediction. The incorporation of the salinity observations in ASSIM also yielded improvements, which are not discussed here.

To investigate skills of FGOALS-g2 in presenting regional SSTA variations on decadal time scale, the Niño3.4 region was selected for study because the SST anomaly (SSTA) in this region defines the ENSO index and affects the countries bordering the Pacific Ocean, i.e., China. As shown in Fig. 6, FGOALS-g2 performed well in simulating the ENSO variation on a decadal time scale in CTRL. FGOALS-g2 had a high correlation coefficient (0.75) with the observation data and a small RMSE (0.142), while the model performed even better in HCST (Fig. 6), with a much higher correlation coefficient (0.90) and a somewhat smaller RMSE (0.107). This significant improvement resulted from the high-quality ICs provided by ASSIM and the dynamic bias correction.

4.4 *Decadal variations of surface air temperature anomaly*

Surface air temperature (SAT) plays a critical role in atmosphere–ocean and atmosphere-land interactions due to its association with heat exchange between the atmosphere and the ocean or land surface (Wang et al., 2009). Its global mean is one of key variables used to describe climate change (e.g., global warming in the past century), and thus this parameter is usually used to evaluate the performance of coupled CSMs. Following the improvements of physical parameterizations, updates of dynamical cores and developments of coupling techniques, the state-of-the-art coupled CSMs have shown strong capability in representing the evolution of globally averaged SAT in the 20th century. This study demonstrates that FGOALS-g2 performs reasonably well at simulating or hindcasting the decadal variations of globally averaged SAT anomaly (SATA) in both CTRL and HCST experiments (Fig. 7). Their correlation coefficients with the observation data were 0.995 and 0.992, respectively. Although the model correlation was somewhat higher in CTRL than in HCST, similar to the results of Keenlyside et al. (2008), the RMSE in CTRL was

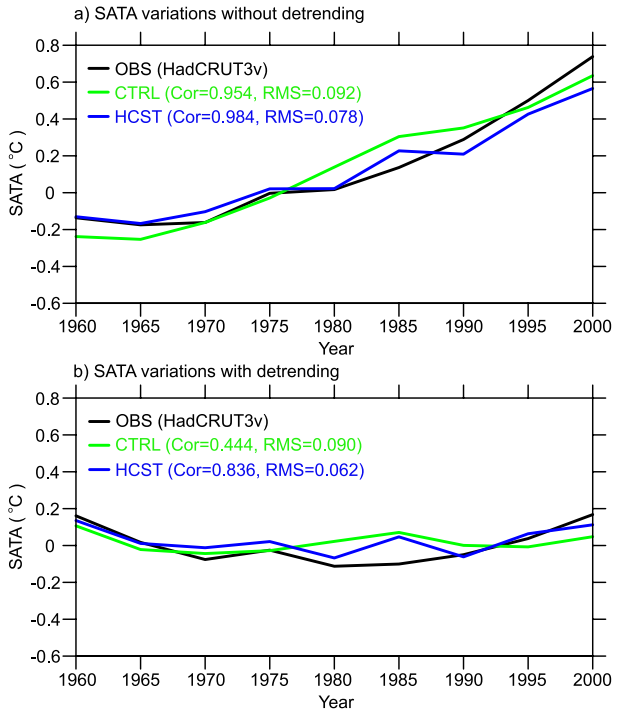

Fig. 8. Decadal variations of regionally averaged surface air temperature (SAT) in China in the observations (black), historic run (green), and hindcast (blue) experiments. The HadCRUT3v dataset (Brohan et al., 2006) was used for the observation data. The units of SAT are °C.

clearly worse than that in HCST. CTRL overestimated global warming after 1980, whereas HCST was closer to the observation data during the same period. The aforementioned characteristics were very similar to those in the decadal variations of global SSTA, which reflects the response of the atmosphere to the ocean in the view of heat exchange.

For the performances of FGOALS-g2 in presenting regional SATA in different experiments, China was chosen as a typical region for evaluations because it has undergone increasing natural disasters (e.g., flood and drought). Under the background of global warming, the regional climate of China has also warmed, which can easily demonstrated by the observational data (Fig. 8a). The model yielded skillful simulations/hindcasts in CTRL and HCST experiments; their correlation coefficients were 0.954 and 0.984, respectively. HCST outperformed CTRL in terms of not only the correlation coefficient but also the RMSE (Fig. 8a). Particularly, significant improvements were found in HCST after detrending (Fig. 8b). In this case, the correlation coefficient between HCST and the observation data was still as high as 0.836, much better than that of CTRL, which was 0.444. Meanwhile, the RMSE of HCST was 0.062, smaller than that of CTRL, which was 0.090.

The better performance of HCST in presenting the SATA over China benefitted from the improvements in decadal variability of SST over the Eastern Pacific and Indian Ocean (Fig. 9, correlation patterns of CTRL and HCST) due to the use of ICs from the initialization. This result can be easily explained: The China climate has a significant monsoon feature that is impacted by the Pacific and Indian Ocean. For example, significant negative correlations between the observed SST and the East Asian summer monsoon (EASM) index from the National Centers for Environmental Prediction (NCEP)/NCAR reanalyses over the tropical central and eastern Pacific and central Indian Ocean were reported by Li et al. (2010); their results indicate the close relationship between weakening of the EASM and warming in both the tropical Pacific and Indian Ocean since 1970s.

Our preliminary evaluations indicate that with better ICs from the initialization and the newly proposed dynamic bias correction, FGOALS-g2 basically performed better at hindcasting than in the historical run in predicting SSTA and SATA, particularly regarding the decadal variations of Niño3.4 SSTA index and regional SATA in China.

5. Summary and conclusions

In this study, a preliminary evaluation of decadal prediction by FGOALS-g2, one of the CMIP5 coupled climate system models mainly developed jointly by

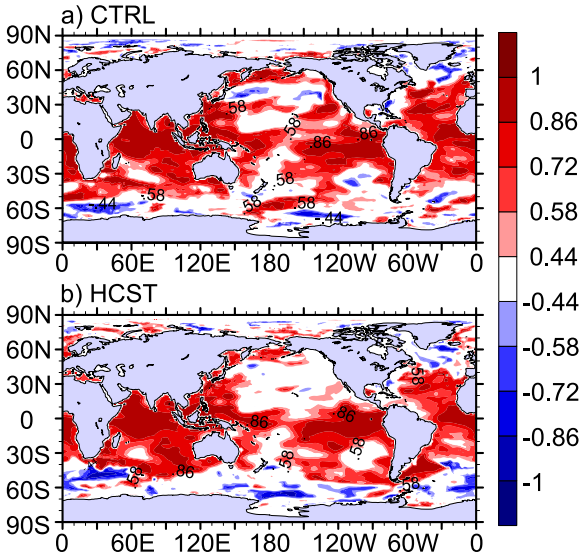

Fig. 9. Correlation patterns between the observed and simulated or hindcasted SST decadal time series at grids for (a) CTRL and (b) HCST, respectively.

LASG/IAP, Chinese Academy of Sciences and CESS, Tsinghua University, was conducted. This evaluation was based on the results from ten sets of 10-year-long, three-member ensemble hindcast experiments performed once five years between 1955 and 2001, one set of 61-year initialization experiments from 1945 to 2005, and one of the historical runs for 20th-century climate simulation from 1850 to 2005. Some datasets were used as the observations, including the ds285.3 analyzed data (Isii et al., 2006), HadCRUT3v (Brohan et al., 2006) and HadISST (Rayner et al., 2003). The hindcast skill of the model on the climatology and mean annual cycle of SST, and decadal variability of SSTA and SATA, particularly the Niño3.4 SSTA index and regional SATA in China, were investigated and compared with those from the historical run and observations. The performance of the nudging-based initialization scheme and the role of the dynamic bias correction scheme in decadal predictions were also examined. Based on the evaluations in this study, following conclusions were formulated:

(1) The overall performance of FGOALS-g2 in the historical run is quite good on decadal variations of SSTA and SATA, although there are overestimations of global warming and global ocean warming after 1980.

(2) The initialization scheme correctly and consistently incorporates the observations into the model integrations and thus provides high-quality ICs for decadal predictions.

(3) The dynamic bias correction scheme proposed in this study shows positive role in alleviating climate drifts and improving hindcast skills.

(4) With the ICs from the initialization and the dynamic bias correction, FGOASL-g2 presents skillful hindcasts on variations of SSTA and SATA on decadal timescale, particularly on decadal variability of ENSO and China SAT. The better performance of HCST on China SAT benefits from the improvements of decadal variability of SST over the Eastern Pacific and Indian Ocean.

Our further evaluations will focus on some typical climate events on decadal timescale, the results of which will be presented in future papers.

Acknowledgements. The first author acknowledges the Ministry of Science and Technology of China for the National High-tech R&D Program (863 Program: Grant No. 2010AA012304) and the National Basic Research Program of China (973 Program: Grant No. 2011CB309704).

REFERENCES

Barnett, T., R. Malone, W. Pennell, D. Stammer, B. Semtner, and W. Washington, 2004: The effects of climate change on water resources in the west: Introduction and overview. *Climatic Change*, **62**, 1–11.

Brohan, P., J. J. Kennedy, I. Harris, S. F. B. Tett, and P. D. Jones, 2006: Uncertainty estimates in regional and global observed temperature changes: A new dataset from 1850. *J. Geophys. Res.*, **111**, D12106, doi: 10.1029/2005JD006548.

Cherupin, G. A., J. A. Carton, and D. Dee, 2005: Forecast model bias correction in ocean data assimilation. *Mon. Wea. Rev.*, **133**, 1328–1342.

Dee, D. P., 2005: Bias and data assimilation. *Quart. J. Roy. Meteor. Soc.*, **131**, 3323–3343.

Ishii, M., M. Kimoto, K. Sakamoto, and S. I. Iwasaki, 2006: Steric sea level changes estimated from historical ocean subsurface temperature and salinity analyses. *Journal of Oceanography*, **62**(2), 155–170.

Keenlyside, N. S., M. Latif, J. Jungclaus, L. Kornblueh, and E. Roeckner, 2008: Advancing dedadal-scale climate prediction in the North Atlantic sector. *Nature*, **453**, 84–88.

Li, H. M., A. G. Dai, T. J. Zhou, and J. Lu, 2010: Responses of East Asian summer monsoon to historical SST and atmospheric forcing during 1950–2000. *Climate Dyn.*, **34**, 501–514.

Li, L. J., X. Xie, B. Wang, and L. Dong, 2012a: Evaluating the performances of GAMIL1.0 and GAMIL2.0 during TWP-ICE with CAPT. *Atmos. Oceanic Sci. Lett.* **5**, 38–42.

Li, L. J., and Coauthors, 2013a: Evaluation of grid-point atmospheric model of IAP LASG, version 2.0 (GAMIL 2.0). *Adv. Atmos. Sci.*, doi: 10.1007/s00376-013-2157-5.

Li, L. J., and Coauthors, 2013b: The flexible global ocean-atmosphere-land system model, grid-point version 2: FGOALS-g2. *Adv. Atmos. Sci.*, doi: 10.1007/s00376-012-2140-6.

Liu, H. L, P. F. Lin, Y. Q. Yu, and X. H. Zhang, 2012: The baseline evaluation of LASG/IAP climate system ocean model (LICOM) version 2.0. *Acta Meteorologica Sinica.*, **26**(3), 318–329, doi: 10.1007/s13351-012-0305-y.

Meehl, G. A., and Coauthors, 2009: Decadal prediction: Can it be skillfull? *Bull. Amer. Meteor. Soc.*, **90**, 1467–1485.

Mochizuki, T., and Coauthors, 2010: Pacific decadal oscillation hindcasts relevant to near-term climate prediction. *PNAS*, **107**, 1833–1837, doi: 10.1073/pnas.0906531107.

Pierce, D. W., T. P. Barnett, R. Tokmakian, A. Semtner, M. Maltrud, J. Lysne, and A. Craig, 2004: The ACPI project, element 1: Initializing a coupled climate model from observed conditions. *Climatic Change*, **62**, 13–28.

Pohlmann, H, J. H. Jungclaus, A. Köhl, D. Stammer, and J. Marotzke, 2009: Initializing decadal climate predictions with the GECCO oceanic synthesis: Effects on the North Atlantic. *J. Climate*, **22**, 3926–3938.

Rayner, N. A., D. E. Parker, E. B. Horton, C. K. Folland, L. V. Alexander, D. P. Rowell, E. C. Kent, and A.

Kaplan, 2003: Global analyses of sea surface temperature, sea ice, and night marine air temperature since the late nineteenth century. *J. Geophys. Res.*, **108**(D14), 4407, doi: 10.1029/2002JD002670.

Schneider, E. K., B. Huang, Z. Zhu, D. G. Dewitt, J. L. Kinter III, B. P. Kirtman, and J. Shukla, 1999: Ocean data assimilation, initialization, and predictions of ENSO with a coupled GCM. *Mon. Wea. Rev.*, **127**, 1187–1207.

Smith, D. M., S. Cusack, A. W. Colman, C. K. Folland, G. R. Harris, and J. M. Murphy, 2007: Improved surface temperature prediction for the coming decade from a global climate model. *Science*, **317**, 796–799.

Troccoli, A., and T. N. Palmer, 2007: Ensemble decadal prediction from analysed initial conditions. *Phil. Trans. Roy. Soc. A*, **365**, 2179–2191.

Wang, B., H. Wan, Z. Z. Ji, X. Zhang, R. C. Yu, Y. Q. Yu, and H. L. Liu, 2004: Design of a new dynamical core for global atmospheric models based on some efficient numerical methods. *Science in China* (*A*), **47**, 4–21.

Wang, B., X. Xie, and L. J. Li, 2009: A review on some aspects of climate simulation evaluation. *Adv. Atmos. Sci.*, **26**(4), 736–747, doi: 10.1007/s00376-009-9038-y.

Wang, X., 2009, Improvements in sea ice component of IAP/LASG climate system model, M.S. thesis, Chinese Academy of Sciences, 101pp. (in Chinese)

Zhang, S., 2011: Impact of observation-optimized model parameters on decadal predictions: Simulation with a simple pycnocline prediction model. *Geophys. Res. Lett.*, **38**, L02702, doi: 10.1029/2010GL046133.